frontiers | Frontiers in Materials

TYPE Original Research
PUBLISHED 19 August 2022
DOI 10.3389/fmats.2022.965674

OPEN ACCESS

EDITED BY
Haibo Kou,
Xi'an University of Science and Technology, China

REVIEWED BY
Yong Deng,
Northwestern Polytechnical University, China
Zhihua Yang,
Harbin Institute of Technology, China

*CORRESPONDENCE
Bi Jia,
Jiabi1127@163.com
Yongjiang Di,
yjdee@163.com

SPECIALTY SECTION
This article was submitted to Smart Materials, a section of the journal Frontiers in Materials

RECEIVED 10 June 2022
ACCEPTED 27 June 2022
PUBLISHED 19 August 2022

CITATION
Zhu J, Jia B, Di Y, Liu B, Wan X, Wang W, Tang R, Liao S and Chen X (2022), Effects of graphene content on the microstructure and mechanical properties of alumina-based composites.
Front. Mater. 9:965674.
doi: 10.3389/fmats.2022.965674

Effects of graphene content on the microstructure and mechanical properties of alumina-based composites

Jun Zhu, Bi Jia*, Yongjiang Di*, Biao Liu, Xin Wan, Wenrong Wang, Rui Tang, Shu Liao and Xingyu Chen

Chongqing Key Laboratory of Nano-Micro Composite Materials and Devices, School of Metallurgy and Materials Engineering, Chongqing University of Science and Technology, Chongqing, China

In this work, alumina-graphene (Al_2O_3-G) composites with graphene contents ranging from 0.5 to 3% were prepared by stepwise feeding ball milling and hot pressing. The influences of graphene content on the microstructure and mechanical properties of Al_2O_3-G composites were investigated. Results showed that the densification, grain sizes, flexural strength, fracture toughness and Vickers hardness of materials increased firstly and then decreased with increasing graphene contents. When the graphene content was 1%, the value of each performance parameter reached the maximum. The average grain size of material decreased from 991 to 551 nm as the graphene content increased from 0 to 1%, but it increased to 863 nm when the graphene content was 3%. The flexural strength, fracture toughness and Vickers hardness of composites with graphene content of 1% increased to 763.5 MPa, 7.4 MPa $m^{1/2}$ and 21.28 GPa. Compared with the Al_2O_3, the fracture strength and toughness of the composites increased by up to 54.63 and 65.54%. Analysis suggested that the strength of Al_2O_3-G composites was mainly related to the grain size and preexisting microflaws.

KEYWORDS

alumina-graphene composites, mechanical properties, microstructure, composites, strength

Introduction

Al_2O_3 ceramics are widely used in machinery manufacturing, national defense and military industry, electronic communications, petrochemicals, etc., owing to their high wear resistance, corrosion resistance, high-temperature resistance and oxidation resistance (Becher and Wei, 1984; Jia et al., 2020; Subbaiah et al., 2021; Vemoori and Khanra, 2021; Zhai et al., 2021; Jiang et al., 2022) However, low toughness and poor thermal shock resistance greatly limit their applications. Therefore, how to improve the toughness of Al_2O_3 ceramics is still a hot spot.

Graphene is a two-dimensional material with large specific surface area, good electrical and thermal conductivity (Lee et al., 2008; Soldano et al., 2010; Novoselov

et al., 2012; Tay and Norkhairunnisa, 2021), which has attracted great attention. The graphene has been used to prepare the Al_2O_3 matrix based composites (Centeno et al., 2013; Chen et al., 2014; Liu et al., 2015; Asiq Rahman et al., 2018). For example, Chen et al. prepared graphene nanosheets reinforced Al_2O_3 matrix based composites by hot pressing (HP), and studied the effect of graphene nanosheets on the microstructure, morphology and mechanical properties of materials (Chen et al., 2014). They found that the fracture toughness of 0.2 wt% graphene nanosheets/alumina composite could reach up to 6.6 MPa $m^{1/2}$ (Chen et al., 2014). Centeno et al. prepared Al_2O_3-G composites by spark plasma sintering (SPS) (Centeno et al., 2013). Liu et al. prepared Al_2O_3-graphene nanosheets composites by SPS, and studied the effects of the addition of graphene on the grain size and mechanical properties of materials (Liu et al., 2015). They reported that the fracture strength and toughness of composites could improve to 708.4 and 3.89 MPa $m^{1/2}$ (Liu et al., 2015), respectively. However, as we know that the graphene is quite difficult to be uniformly dispersed in the Al_2O_3 matrix, the agglomeration of graphene would cause defects such as microflaws and micropores in the matrix (Hu et al., 2016; Kostecki et al., 2016). The dispersion of graphene has always been a difficult point.

In the previous work (Zhang et al., 2022), we designed a method called stepwise feeding ball milling to better achieve the dispersion of graphene in Al_2O_3 matrix, and studied the mechanical properties of Al_2O_3-1.0 wt% graphene composites. The fracture strength and fracture toughness of composites reached 754.20 and 7.50 MPa $m^{1/2}$ (Zhang et al., 2022). In this work, in order to systematically study the effect of the added graphene content on the microstructure and mechanical properties of the material, we prepared the Al_2O_3-G composites with graphene contents ranging from 0.5 to 3% by using the stepwise feeding ball milling and hot pressing. The restively density, microstructures and mechanical properties of composites were evaluated and compared.

Experimental process

Materials

The Al_2O_3 powder (Hangzhou Wanjing New Materials Co., Ltd., 0.5 μm) and graphene powder (Wuxi Nadun Technology Co., Ltd., 1 μm) were used as raw materials. Absolute alcohol (Wuxi Nadun Technology Co., Ltd.) was used as dispersing agent in ball milling. All chemicals were used as received without further purification.

Fabrication of Al_2O_3-G composites

To enhance the desperation of graphene, the Al_2O_3-G composites were prepared by a novel feeding method called stepwise feeding ball milling that we reported in our previous work (Zhang et al., 2022). As shown in Figure 1, the graphene powder was firstly added into the ball mill respectively, followed by Al_2O_3 powder and zirconia balls in a 1:2 weight ratio. The mixed powders were milled in 200 g absolute ethanol at 90 rpm min-1, and then 200 g ethanol was continued to be added after ball milling for 5 h; then other 400 g ethanol was added after ball milling for 4 h. Until the mixed powders presented a paste state, another 400 g ethanol was added, and then the mixture were continued to grind for 40 h to obtain the slurry. After grinding, the slurry was dried at a temperature of 50°C for 12 h, and then were sieved through a 80-mesh sieve. Finally, the prepared powders were hot-pressed at 1,550°C, 40 MPa for 60 min to gain the Al_2O_3-G composite with graphene contents ranging from 0.5 to 3%.

After cutting, rough grinding and fine grinding, the prepared Al_2O_3-G composite samples were made into standard samples of 35 mm × 4 mm × 3 mm for characterization.

Material characterization

The relative densities of Al_2O_3-G composites were measured by the Archimedes method with deionized water as the immersing medium. In order to determine their relative density, the theoretical density of the nanocomposites was calculated by the volume-based rule of mixtures assuming densities of 3.96 g/cm^3 and 2.1 g/cm^3 for Al_2O_3 and graphene, respectively (Vemoori and Khanra, 2021).

The microstructure, fracture morphology, and interface bonding of etch composites were observed by scanning electron microscopy (SEM; JSM-7800F, at 10 kV). The compositions and elemental distributions of the Al_2O_3-G composites were analyzed using an energy dispersive X-ray spectrometry (EDS; JSM-7800F). All Samples were prepared for microscopy by cutting cross sections parallel to the hot-pressing direction and then polishing to a 0.30 μm finish using diamond abrasives. The phase composition of the Al_2O_3-G composites was analyzed using X-ray diffraction (XRD; XRD-7000S/L). The average grain size of composite was measured by Image J (Image J; US National Institutes of Health, Bethesda, MD) by counting a minimum of 100 grains. The longest diameter of the grain was reported as the average grain size.

Mechanical testing

Hardness of the samples was determined by Vickers indentation (452SVD, China) using the load of 10 kg and the dwell time was 15s. Reported values were obtained from an average of 5 indentations on a single specimen.

Universal testing machine (UH6104A, China) was used to check the bending strength and fracture toughness of the

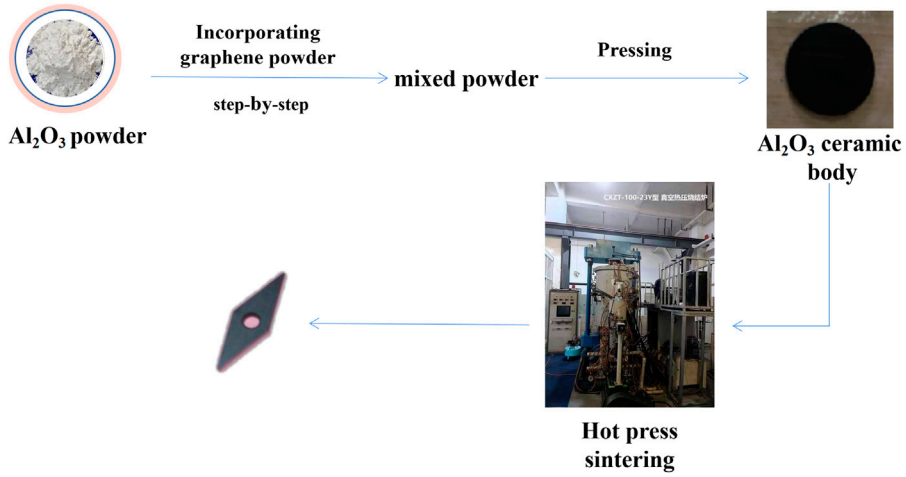

FIGURE 1
The schematic of preparation process of Al_2O_3-G composites.

samples. The bending strength was characterized by the three-point bending test with 0.5 mm/min loading rate. The size of bending specimen is 3 × 4 × 35 mm, and the span is 30 mm. The fracture toughness of the samples (specimen size was 3 × 4 × 35 mm, notched size was 2 mm) was measured by the single-edge-v-notched beam (SEVNB) method.

Results and discussion

The crystal structure and surface morphology of Al_2O_3-G composites with different graphene content were tested by XRD and SEM, respectively. Figure 2A shows the XRD patterns of Al_2O_3-G composites. It can be seen from the figure that when 2θ is 25.58°, 35.15°, 37.79°, 43.37°, 46.20°, 52.57°, 57.51°, 61.15°, 66.54°, 68.24°, 76.88° and 77.25°. There are obvious diffraction peaks, and each diffraction peak is basically consistent with the α-Al_2O_3 spectrum in JCPDS 74–1,081, showing that the Al_2O_3-G composite is α-Al_2O_3 phase (Li et al., 2016). When the graphene content in the matrix is 0wt% and 0.5wt%, only α-Al_2O_3 exists in the composite, and the peak of graphene is not obvious as the content of graphene is relatively small (Ahmad et al., 2015; Li et al., 2016). When the graphene content is higher than 1.0 wt%, an obvious diffraction peak appears at 26.5° corresponds to the (002) crystal plane of graphene, indicating that the graphene has been successfully introduced into the Al_2O_3 matrix and has no significantly effect on the crystal phase of Al_2O_3.

Figures 2B–F show the surface morphology of Al_2O_3-G composites with 0, 0.5, 1, 1.5, 3.0 wt% graphene content, respectively. As shown in Figure 2B, the crystalline grains of pure alumina ceramics are coarse and the boundaries of crystalline grains is not obvious. Moreover, many pores exist in pure alumina ceramics, which may result in the decreasing of density. With the increasing of graphene content, the grain size of the Al_2O_3-G composite first decreases and then increases obviously (Figures 2B–F). When the content of graphene rises to 1.0 wt%, the grain size of composite is smallest (551 nm), which is reduced by 55.6% compared with the pure Al_2O_3. The reason may be that graphene is located at the boundary of grain, which hinders the movement of the grain boundary and inhibits the growth of the matrix grains (Ahmad et al., 2015), thereby refining the grains. However, when the graphene content exceeds 1.0 wt%, the grain size increases again. When the graphene content is 3.0 wt%, the grain size of composite reaches 863 nm. There is an obvious agglomeration phenomenon, which may be due to the strong van der Waals force between the graphene itself. When the graphene content is higher, it has a poor compatibility with the Al_2O_3-G composite and unevenly disperses in the matrix, leading to the increase of grain size, which may affect the mechanical properties of composite (Li et al., 2016).

Table 1 shows the content distribution of Al, O and C element in Al_2O_3-G composites with different graphene contents. The atomic ratio of Al and O element in the samples is close to 2:3, which agrees with the stoichiometry of Al_2O_3. Clearly, with increasing graphene content, the proportion of Al and O atoms in the sample does not change significantly, while the proportion of C rises obviously. When the graphene content increases up to 3.0 wt%, the atomic ratio of C is 38.5%, indicating that the surface coverage of C is very high and which may reduce the performance of Al_2O_3-G composite.

To identify the influence of graphene content on the grain size of Al_2O_3-G composite, the average grain degrees is carefully analyzed, and the results are shown in Table 2. Clearly, with

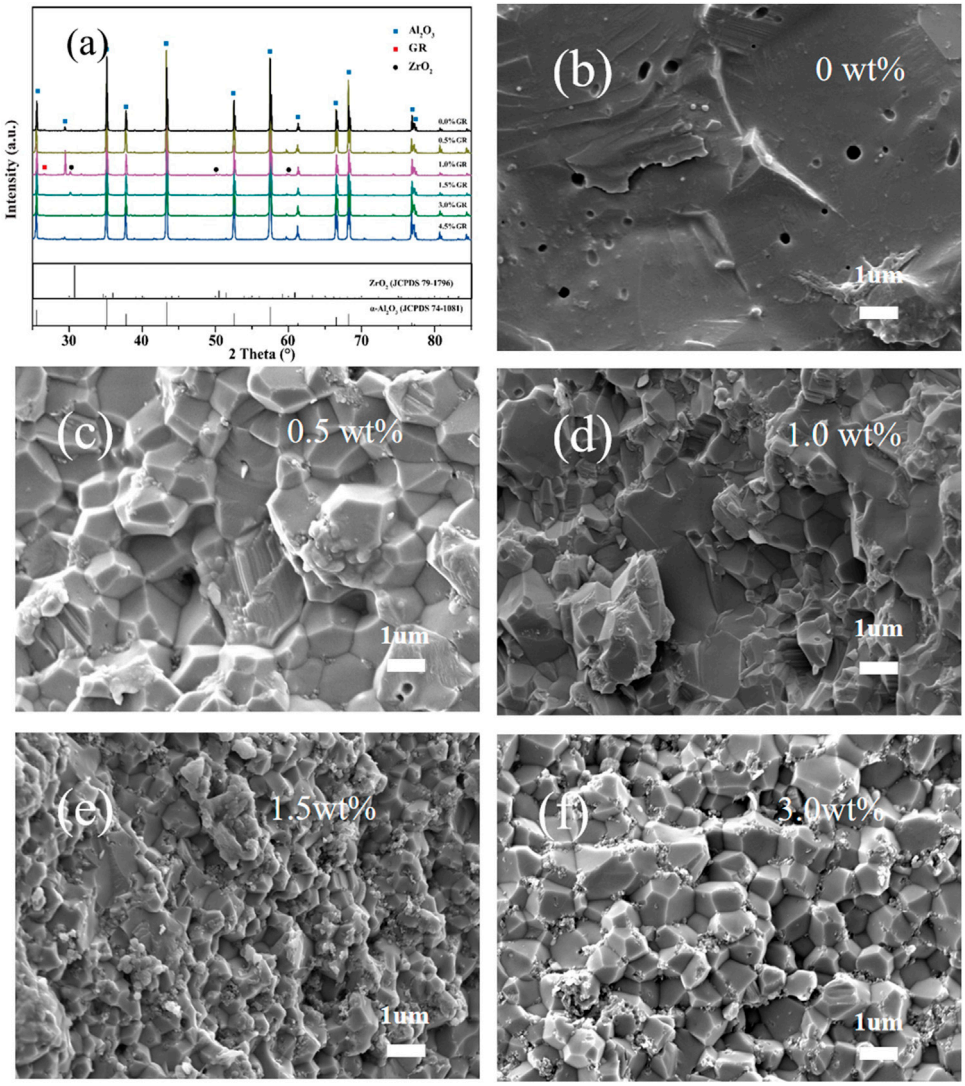

FIGURE 2
(A) XRD patterns of Al_2O_3-G composites with different content of graphene; **(B–F)** SEM images of Al_2O_3-G composites with different graphene contents.

TABLE 1 Contents of Al, O and C in Al_2O_3-G composites with different graphene contents.

	Al (at%)		O (at%)		C (at%)	
	Theory	EDS test	Theory	EDS test	Theory	EDS test
0.0 wt%	40.0	40.2	60.0	59.8	0.0	0.0
0.5 wt%	38.4	36.6	57.5	54.4	4.1	9.1
1.0 wt%	38.2	32.1	57.3	48.3	8.2	19.6
1.5 wt%	38.0	28.5	57.0	41.7	12.3	29.8
3.0 wt%	37.4	24.3	56.1	37.1	24.6	38.5

TABLE 2 Average grain degrees of Al_2O_3-G composites with different graphene contents.

Graphene content/wt%	D_{hkl} (nm)
0	991
0.5	983
1.0	551
1.5	673
3.0	863

increasing graphene content, the average grain size of Al_2O_3-G composites decreases firstly and then increases, which is consistent with the phenomenon observed in Figure 2. When the content rises to 1.0 wt%, the grain size reaches a minimum value of 551 nm, which is 55.60% smaller than the average grain size of pure Al_2O_3. While the graphene content rises to 3.0 wt%, the grain size reaches 883 nm, showing that the appropriate content of graphene can significantly reduce the grain size, while the excessive graphene content has no obvious effect on grain refinement.

Figure 3 shows the relative density, bending strength, fracture toughness and Vickers hardness of Al_2O_3-G composites as a function of graphene content. The results show that the density, bending strength, fracture toughness and Vickers hardness of materials increase firstly and then decrease with increasing graphene contents. When the graphene content reaches up to 1%, the value of each performance parameter reaches the maximum. The relative density, bending strength, fracture toughness and Vickers hardness of Al_2O_3-1.0 wt% graphene composites increase to 99.4%, 763.5 MPa, 7.4 MPa $m^{1/2}$ and 21.28 GPa, respectively. Compared with the Al_2O_3, the fracture strength and toughness of the composites increase by up to 54.63 and 65.54%.

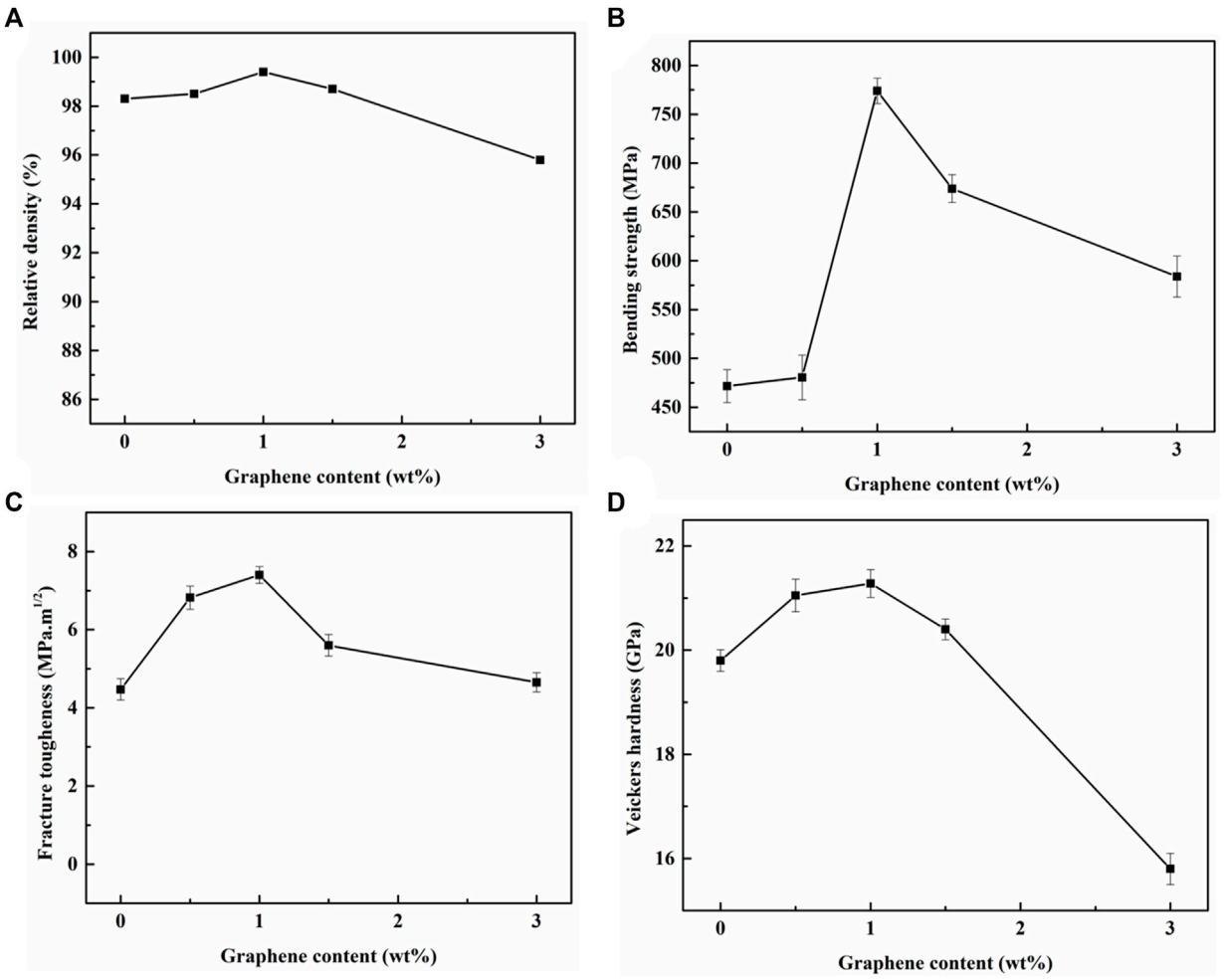

FIGURE 3
Variation curves of **(A)** relative density, **(B)** bending strength, **(C)** fracture toughness and **(D)** Vickers hardness of Al_2O_3-G composites with graphene contents.

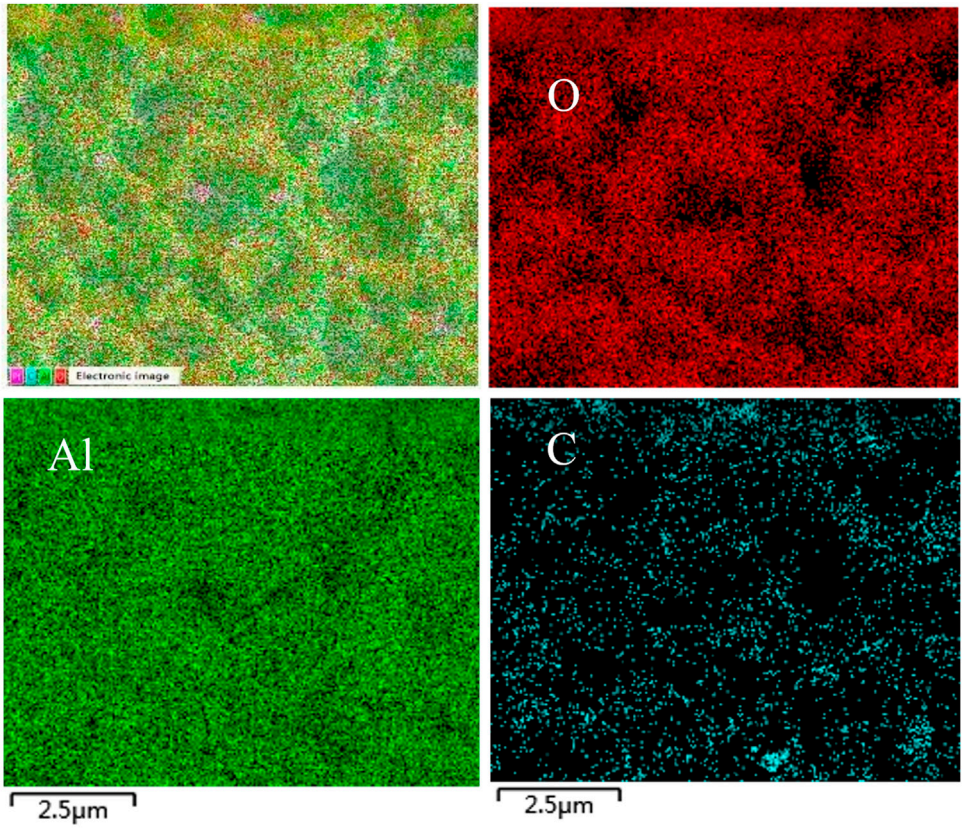

FIGURE 4
EDS element distribution map of Al_2O_3-1.0 wt% graphene composites.

Figure 4 shows the EDS element distribution map of Al_2O_3-1.0 wt% graphene composites. It can be seen from the figure that Al, O, and C elements are uniformly distributed, indicating that the graphene is evenly distributed in the matrix, and there is no obvious agglomeration phenomenon. The added graphene on the grain boundary of Al_2O_3 hinders the migration of grain boundary and inhibits the growth of grains during the sintering process, thereby refining the grain sizes and increasing the relative density of composites (Cheng et al., 2017). However, with the further increase of graphene content, the excessive graphenes are difficult to distribute evenly at the grain boundary, and which are prone to agglomeration. This results in the generation of micro flaws and pores (as shown in Figures 2E,F), leading to the decrease of density.

According to the Griffith fracture theory, the fracture strength of brittle materials is controlled by the critical flaw size, which can be expressed as follows

$$\sigma_f = \sqrt{\frac{2E\gamma}{\pi a}} \tag{1}$$

where σ_f is the fracture strength of materials; E is the Young's modulus of materials; γ is the fracture surface energy of materials; a is the critical flaw size of materials. The studies showed that the critical flaw size of ceramics is related to the grain size and the size of microflaw around the grain (Krstic, 2006; Rezaie et al., 2007). Then, Eq. 1 can be modified as

$$\sigma_f = \sqrt{\frac{2E\gamma}{\pi(R+s)}} \tag{2}$$

In Eq. 2, R is the grain size, and s is the size of flaw around the grain. Meanwhile, the preexisting microflaws and micropores could reduce the densification of materials, and then reduce the Young's modulus of materials, followed by the decreasing of the fracture strength of materials (Krstic, 2006). According to Figure 2 and Table 2, Al_2O_3-1.0 wt% graphene composite has a smaller grain size, and no obvious micro flaws and pores are found, compared to the Al_2O_3-G composites with other graphene contents. Then, it can be concluded that when the graphene content is less than 1, the strength of composites should increase with increasing graphene content. While the strength of composites will decrease with the further increase of graphene content. This is completely consistent

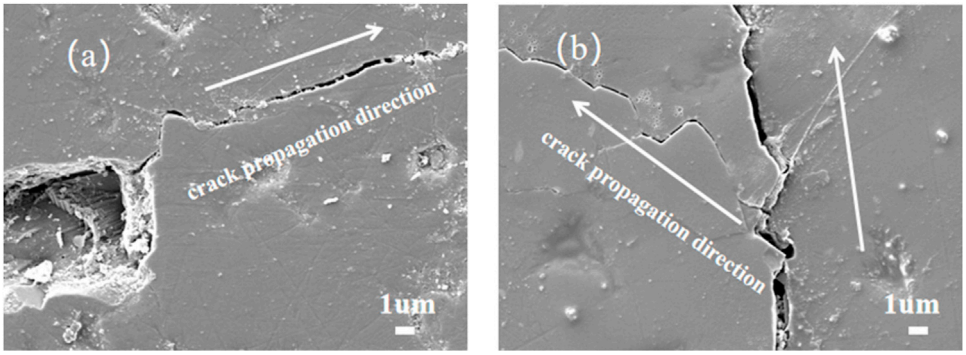

FIGURE 5
SEM images of crack propagation path of **(A)** Al_2O_3 and **(B)** Al_2O_3-1.0 wt% graphene composites.

with the experimental phenomenon. The hardness and fracture toughness are also controlled by the critical flaw including grain, preexisting microflaws and micropores (Wang et al., 2019; Wang et al., 2021a; Wang et al., 2021b). Figure 2 shows that the fracture mode of Al_2O_3 is mainly intergranular fracture. After adding graphene, the fracture mode of composites appears transgranular fracture, and the proportion shows an increasing trend. The graphene makes the bonding between grains tighter and increases the bonding energy of grain boundaries, so that some cracks tend to move through grains rather than along grain boundaries during propagation (Porwal et al., 2013; Iftikhar et al., 2016), These changes in fracture behavior consume more strain energy and increase the fracture toughness of Al_2O_3. At the same time, the observed pull-out of graphene also increases the fracture toughness of the material.

Figure 5 shows the SEM images of indentation crack propagation path of Al_2O_3 and Al_2O_3-1.0 wt% graphene composites. It can be seen that the crack propagation path of Al_2O_3 is almost straight, and there is only one main crack. While for that of the Al_2O_3-1.0 wt% graphene composites, due to the hindering effect of graphene, crack deflection, crack bifurcation and bridging appear during the crack propagation process. These behaviors require more strain energy to drive crack propagation, thereby increasing the material's resistance to crack propagation.

Conclusion

In this work, the Al_2O_3-G composites with graphene contents ranging from 0.5 to 3% were prepared by stepwise feeding ball milling and hot pressing. The density, bending strength, fracture toughness and Vickers hardness of materials increased firstly and then decreased with increasing graphene contents. When the graphene content reached up to 1%, the density, bending strength, fracture toughness and Vickers hardness of Al_2O_3-1.0 wt% graphene composites increased to 99.4%, 763.5 MPa, 7.4 MPa $m^{1/2}$ and 21.28 GPa, respectively. The fracture strength and toughness of the composites increased by up to 54.63 and 65.54% compared to that of the Al_2O_3. Results showed that the strength of composites is mainly controlled by the grain, preexisting microflaws and micropores. The fracture toughness of composites is improved by the change in fracture mode, pull-out of graphene, crack deflection, crack bifurcation and bridging.

Data availability statement

The original contributions presented in the study are included in the article/Supplementary Material, further inquiries can be directed to the corresponding authors.

Author contributions

JZ: Investigation; Methodology; Data analysis; Writing of original draft. BJ: Funding acquisition; Investigation; Methodology; Data analysis; Writing of original draft; Writing of review and editing. YD: Investigation; Methodology; Data analysis; Writing of review and editing. BL: Investigation; Data analysis; Writing of original draft. XW: Data analysis; Writing of review and editing. WW: Data analysis; Writing of review and editing. RT: Investigation; Data analysis; Writing of original draft. SL: Data analysis; Writing of original draft. XC: Data analysis; Writing of original draft.

Funding

This work was supported by the National Natural Science Foundation of China under Grant No. 11972100, and the Natural

Science Foundation Project of CQ CSTC under Grant No. cstc2019jscx-fxydX0075.

Conflict of interest

The authors declare that the research was conducted in the absence of any commercial or financial relationships that could be construed as a potential conflict of interest.

Publisher's note

All claims expressed in this article are solely those of the authors and do not necessarily represent those of their affiliated organizations, or those of the publisher, the editors and the reviewers. Any product that may be evaluated in this article, or claim that may be made by its manufacturer, is not guaranteed or endorsed by the publisher.

References

Ahmad, I., Islam, M., and Abdo, H. S. (2015). Toughening mechanisms and mechanical properties of graphene nanosheet-reinforced alumina. *Mater Des.* 88 (12), 34–43. doi:10.1016/j.matdes.2015.09.125

Asiq Rahman, O. S., Sribalaji, M., Mukherjee, B., Laha, T., and Keshri, A. K. (2018). Synergistic effect of hybrid carbon nanotube and graphene nanoplatelets reinforcement on processing, microstructure, interfacial stress and mechanical properties of Al2O3 nanocomposites. *Ceram. Int.* 44, 2109–2122. doi:10.1016/j.ceramint.2017.10.160

Becher, P. F., and Wei, G. C. (1984). Toughening behavior in SiC-whisker-reinforced alumina. *J. Am. Ceram. Soc.* 67, 267–269. doi:10.1111/j.1151-2916.1984.tb19694.x

Centeno, A., Rocha, V. G., Alonso, B., Fernández, A., Gutierrez-Gonzalez, C. F., Torrecillas, R., et al. (2013). Graphene for tough and electroconductive alumina ceramics. *J. Eur. Ceram. Soc.* 33, 3201–3210. doi:10.1016/j.jeurceramsoc.2013.07.007

Chen, Y.-F., Bi, J.-Q., Yin, C.-L., and You, G.-L. (2014). Microstructure and fracture toughness of graphene nanosheets/alumina composites. *Ceram. Int.* 40, 13883–13889. doi:10.1016/j.ceramint.2014.05.107

Cheng, Y., Zhang, Y., Wan, T., Yin, Z., and Wang, J. (2017). Mechanical properties and toughening mechanisms of graphene platelets reinforced Al2O3/TiC composite ceramic tool materials by microwave sintering. *Mater. Sci. Eng. A* 680, 190–196. doi:10.1016/j.msea.2016.10.100

Hu, Y. Y., Xu, C. H., Xiao, C. G., and Yi, M. D. (2016). Preparation and properties of alumina/graphene oxide composite ceramics. *J. Silic.* 44, 432–437. doi:10.14062/j.issn.0454-5648.2016.03.14

Iftikhar, A., Mohammad, I., Tayyab, S., and Zhu, Y. Q. (2016). Toughness enhancement in graphene nanoplatelet/SiC reinforced Al_2O_3 ceramic hybrid nanocomposites. *Nanotechnology* 27, 425704. doi:10.1088/0957-4484/27/42/425704

Jia, B., Li, X. B., Pan, F. S., Wang, R. Z., and Yuan, Y. J. (2020). The effect of hotpressing sintering temperature on graphene-reinforced alumina matrix composites. *Mater. Rev.* 34, 24001–24004. doi:10.11896/cldb.19120144

Jiang, D., Qin, J., Zhou, X., Li, Q., Yi, D., and Wang, B. (2022). Improvement of thermal insulation and compressive performance of Al2O3-SiO2 aerogel by doping carbon nanotubes. *Ceram. Int.* 48, 16290–16299. doi:10.1016/j.ceramint.2022.02.178

Kostecki, M., Grybczuk, M., Klimczyk, P., Cygan, T., Woźniak, J., Wejrzanowski, T., et al. (2016). Structural and mechanical aspects of multilayer graphene addition in alumina matrix composites-validation of computer simulation model. *J. Eur. Ceram. Soc.* 36, 4171–4179. doi:10.1016/j.jeurceramsoc.2016.06.034

Krstic, V. D. (2006). Effect of microstructure on fracture of brittle materials: Unified approach. *Theor. Appl. Fract. Mech.* 45, 212–226. doi:10.1016/j.tafmec.2006.03.005

Lee, C., Wei, X., Kysar, J. W., and Hone, J. (2008). Measurement of the elastic properties and intrinsic strength of monolayer graphene. *Science* 321, 385–388. doi:10.1126/science.1157996

Li, H. Z., Li, Z. J., Luo, X. D., Li, X. W., and Xie, Z. P. (2016). Effect of CeO_2 on microstructure of mollaite ceramics. *Mater. Guide* 30, 452–455.

Liu, X., Fan, Y.-C., Li, J.-L., Wang, L.-J., and Jiang, W. (2015). Preparation and mechanical properties of graphene nanosheet reinforced alumina composites. *Adv. Eng. Mat.* 17, 28–35. doi:10.1002/adem.201400231

Novoselov, K. S., Fal′ko, V. I., Colombo, L., Gellert, P. R., Schwab, M. G., and Kim, K. (2012). A roadmap for graphene. *Nature* 490, 192–200. doi:10.1038/nature11458

Porwal, H., Tatarko, P., Grasso, S., Khaliq, J., Dlouhý, I., and Reece, M. J. (2013). Graphene reinforced alumina nano-composites. *Carbon* 64, 359–369. doi:10.1016/j.carbon.2013.07.086

Rezaie, A., Fahrenholtz, W. G., and Hilmas, G. E. (2007). Effect of hot pressing time and temperature on the microstructure and mechanical properties of ZrB2-SiC. *J. Mater Sci.* 42, 2735–2744. doi:10.1007/s10853-006-1274-2

Soldano, C., Mahmood, A., and Dujardin, E. (2010). Production, properties and potential of graphene. *Carbon* 48, 2127–2150. doi:10.1016/j.carbon.2010.01.058

Subbaiah, G. B., Ratnam, K. V., Janardhan, S., Shiprath, K., Manjunatha, H., Ramesha, M., et al. (2021). Metal and metal oxide based advanced ceramics for electrochemical biosensors-A short review. *Front. Mat.* 8, 682025. doi:10.3389/fmats.2021.682025

Tay, C. H., and Norkhairunnisa, M. (2021). Mechanical strength of graphene reinforced geopolymer nanocomposites: A review. *Front. Mat.* 8, 661013. doi:10.3389/fmats.2021.661013

Vemoori, R., and Khanra, A. K. (2021). Microstructural and mechanical properties of Al2O3 and ZTA foams prepared by thermo-foaming technique. *Ceram. Int.* 47, 29881–29887. doi:10.1016/j.ceramint.2021.07.161

Wang, R., Li, D., and Li, W. (2021). Temperature dependence of hardness prediction for high-temperature structural ceramics and their composites. *Nanotechnol. Rev.* 10, 586–595. doi:10.1515/ntrev-2021-0041

Wang, R., Li, D., Wang, X., and Li, W. (2019). Temperature dependent fracture toughness of the particulate-reinforced ultra-high-temperature-ceramics considering effects of change in critical flaw size and plastic power. *Compos. Part B Eng.* 158, 28–33. doi:10.1016/j.compositesb.2018.09.049

Wang, R., Wang, S., Li, D., Xing, A., Zhang, J., Li, W., et al. (2021). Theoretical characterization of the temperature dependence of the contact mechanical properties of the particulate-reinforced ultra-high temperature ceramic matrix composites in Hertzian contact. *Int. J. Solids Struct.* 214-215, 35–44. doi:10.1016/j.ijsolstr.2021.01.005

Zhai, S., Liu, J., and Liu, Q. (2021). Changes in the microstructure and mechanical properties of Al2O3/YSZ directionally solidified eutectic ceramics during long-time heat treatment. *J. Eur. Ceram. Soc.* 41, 266–273. doi:10.1016/j.jeurceramsoc.2021.09.026

Zhang, D. H., Wu, X. Q., Jia, B., Jiang, H. M., and Liu, Y. (2022). Effects of preparation methods on the microstructure and mechanical properties of graphene-reinforced alumina matrix composites. Submitted to the journal of Materials.